

UNCLASSIFIED

AD-A277 064



AR-008-170



DEPARTMENT OF
DEFENCE

DSTO

**Land, Space and
Optoelectronics Division**

TECHNICAL REPORT
SRL-0130-TR

ANALYSIS AND COMPENSATION FOR WINDOW ALIGNMENT
ERRORS IN AN UNDERWATER STEREO TV CAMERA
RANGING AND SIZING SYSTEM

by

S.J. Sutherland

DTIC
ELECTE
MAR 21 1994

94-08744



APPROVED FOR PUBLIC RELEASE

UNCLASSIFIED

DTIC QUALITY ASSURED 1

SURVEILLANCE RESEARCH LABORATORY

94 3 18 012

UNCLASSIFIED

AR-008-170



SURVEILLANCE RESEARCH LABORATORY

Land, Space and Optoelectronics Division

TECHNICAL REPORT
SRL-0130-TR

ANALYSIS AND COMPENSATION FOR WINDOW ALIGNMENT
ERRORS IN AN UNDERWATER STEREO TV CAMERA
RANGING AND SIZING SYSTEM
by

S.J. Sutherland

Accession For	
NTIS	CRA&I <input checked="checked" type="checkbox"/>
DTIC	TAB <input type="checkbox"/>
Unannounced <input type="checkbox"/>	
Justification	
By	
Distribution /	
Availability Codes	
Dist	Avail and/or Special
A-1	

SUMMARY

This report considers the theoretical analysis of measurement errors introduced in an underwater stereopsis system which has front window misalignment. It develops new range and size equations and models the effects of window misalignment, range equation approximation and system sampling effects. A scheme is given which will allow underwater calibration in a practical system. The report concludes that the new range and size equations developed provide enhanced accuracy to a point where the system sampling effects become the dominant source of error.

© COMMONWEALTH OF AUSTRALIA 1993

OCT 93

APPROVED FOR PUBLIC RELEASE

POSTAL ADDRESS: Director, Surveillance Research Laboratory, PO Box 1500, Salisbury, South Australia, 5108. **SRL-0130-TR**

UNCLASSIFIED

This work is Copyright. Apart from any fair dealing for the purpose of study, research, criticism or review, as permitted under the Copyright Act 1968, no part may be reproduced by any process without written permission. Copyright is the responsibility of the Director Publishing and Marketing, AGPS. Inquiries should be directed to the Manager, AGPS Press, Australian Government Publishing Service, GPO Box 84, Canberra ACT 2601.

CONTENTS

	Page No.
1. Introduction.....	1
2. Derivation of Range and Size Formulae	1
2.1. Simple Range and Size Formulae	1
2.2. Range and Size Formulae with Window Misalignment	2
3. System Calibration.....	4
4. System Modelling	4
4.1. Simple Range Equation.....	4
4.2. Full Range and Size Formulae	5
4.3. Range and Size Formula Approximations	5
4.4. Sampling Effects.....	6
4.5. Effect of Range Calculation on Size Measurement	6
5. Conclusions.....	7
6. Acknowledgments	7
References.....	9
Figure 1 - Ranging with Stereo TV Cameras	11
Figure 2a - Simplified Ranging System.....	12
Figure 2b - Simple Size Measurement	12
Figure 3 - System with Window Misalignment.....	13
Figure 4 - Size Measurement.....	14
Figure 5 - Calibration Chart.....	15
Figure 6 - System Calibration	16
Figure 7 - Calculated Range & Size for the Simple Formula	17
Figure 8 - Range & Size Calculations for Full Formula	18
Figure 9 - Comparison of Range Results	19
Figure 10 - Range Calculation with Two Sample Sizes	20
Figure 11 - Effect of Calculated Range Inaccuracy on the Size Calculation	21
Appendix A - Theoretical Development of the Optical Effects of Window Misalignment in a three Media System	23
Appendix B - Derivation of Range and Size Formulae to include misalignment Errors.....	27

SRL-0130-TR

UNCLASSIFIED

1. INTRODUCTION

The principle of using a pair of similar TV cameras to derive the range and size of viewed objects is well known [1,2]. This report analyses and describes a problem caused by front window misalignment in a real underwater stereo ranging system and presents a way to compensate for the range and size measurement errors which occur. Whilst previous work has looked at compensating for optical distortions [3] such schemes are often impractical in a real-time system and do not consider the effects of a water medium in front of the camera. One paper which has looked at underwater photogrammetry [4] does not examine the effects upon a stereoscopic system, nor does it consider the effects of window misalignment. This paper represents a pragmatic approach to a specific problem with a solution which is achievable in real-time and with a calibration scheme which may be performed underwater.

Figure 1 shows a typical system in which the range of an object seen by both cameras may be determined using triangulation. Once the range is known the object size may be determined by using the range as a scaling factor.

With an air medium between the objects and cameras the range and size calculations are fairly straightforward but when the medium is water other effects become apparent. Previous experience with underwater stereopsis has revealed a problem with camera alignment. It was found that after aligning the two cameras in air (for parallel optical axes) they became optically misaligned when submerged. It was suspected that this effect was due to a misalignment (or 'tilt') of the front window of the cameras' water-tight housings relative to the cameras' optical axes. Corena and Gillyon [5] modelled the arrangement by ray tracing and were able to show that a constant angular offset in the principal ray of the order of those observed (around 0.3°) will occur with front window tilts of around 1° . These misalignments may occur during manufacture, assembly or during use and there is usually no convenient means of correction.

This report considers the effect of these misalignments on the system ranging performance. First the normal range equation is derived and then extended to take account of misalignment errors. Next, the way in which an underwater calibration may be used to reduce the effects of misalignment is given. Following on from this, the results of system simulations for various formulations of the ranging calculation are presented to illustrate how the gross effects of misalignment may be taken into account and appropriate compensation made. These simulations include the effects of camera focal plane sampling to assess the contribution which this makes to the range and size calculation accuracy.

2. DERIVATION OF RANGE AND SIZE FORMULAE

2.1. Simple Range and Size Formulae

This section gives the derivation of the simple range and size formulae in which no account is taken of window misalignment. The calculations are based around an optical system of the type given in Figure 2a. Note that anticlockwise angles are positive and the coordinate system origin lies on the left camera optical axis at the lens centre.

From this diagram we have :-

$$B = O_1 - O_2$$

$$= R \tan \alpha_2 - R \tan \alpha_1$$

where B is the cameras' baseline length
 R is the object's range.

$$\text{So, } R = \frac{B}{\tan \alpha_2 - \tan \alpha_1} \quad (1)$$

$$R = \frac{fB}{i_2 - i_1} \quad *$$

where f is the cameras' focal length
 i_1 and i_2 are the left and right camera image positions for the object.

In practice i_1 and i_2 are measured from the TV picture, often by overlaying the left and right images and allowing an operator to 'merge' the two images of the object being ranged. The amount of shifting of the images relates to $(i_2 - i_1)$.

To derive the size formula we begin with (from Figure 2b) :-

$$S = O_2 - O_1$$

where S is the object size.

$$= R \tan \alpha_2 - R \tan \alpha_1$$

$$S = R(\tan \alpha_2 - \tan \alpha_1)$$

Now,

$$\tan \alpha_1 = \frac{i_1}{f} \quad \text{and likewise for } \tan \alpha_2. \text{ So we can say :-}$$

$$S = \frac{R}{f} (i_2 - i_1) \quad (3)$$

where i_1 and i_2 are the image positions for the object sizing points

These are the commonly used formulations of the range and size calculations. We will now consider the effects of window misalignment.

2.2. Range and Size Formulae with Window Misalignment

As discussed above, underwater systems are known to have errors introduced by misalignment of the front window of the water-tight housing. Appendix A provides a theoretical development which demonstrates how a fixed window tilt will produce a fixed angular offset in any ray. This angular offset will be approximately equal to one third the window tilt and in the opposite direction. The appendix also shows how the translational shift in a ray will be negligible. Thus we make the assumption of a fixed tilt error during our development of the new range and size equations.

* All derivations used in this report assume a camera focused at infinity and therefore use focal length and image distance interchangeably. For a typical lens of 8 mm focal length this results in errors of 0.08% for a camera focussed at 10 m and 0.8% for a camera focussed at 1 m.

Figure 3 shows a stereopsis system with window misalignment. Note that angular offsets are positive anticlockwise.

Whilst equation (1) holds true, equation (2) does not, since the image positions are no longer solely dependent upon the object position and the lens focal length. Hence we need to derive the range and size equations for this more realistic system model. Appendix B gives the derivations of these equations which are simply stated here. For the range :-

$$R = \frac{B \left(f + i_l \Delta_r + i_r \Delta_l + \frac{i_l i_r \Delta_l \Delta_r}{f} \right)}{i_l - i_r + f(\Delta_r - \Delta_l) + \frac{i_l i_r (\Delta_r - \Delta_l)}{f} + \Delta_l \Delta_r (i_l - i_r)} \quad (4)$$

where Δ_l and Δ_r are the left and right camera tilts in the horizontal plane

We will show below how $(\Delta_r - \Delta_l)$ may be measured by performing a calibration. In a practical, in-service system it would be extremely difficult to measure Δ_l and Δ_r independently and so we would like to be able to ignore terms in which they occur independently in order that we might use the approximation :-

$$R \approx \frac{Bf}{i_l - i_r + f(\Delta_r - \Delta_l) + \frac{i_l i_r (\Delta_r - \Delta_l)}{f}} \quad (5)$$

in which all terms are either known or are measurable. We will show later by simulation the effects of ignoring these terms.

Again referring to appendix B and Figure 4, the size formula is :-

$$S = R \left(\frac{i_2 i_1 + \Delta_r^2 (i_2 - i_1)}{f + \Delta_r (i_1 + i_2) + \frac{i_1 i_2 \Delta_r^2}{f}} \right) \quad (6)$$

Since the Δ_r term is not readily measured in practice, we would like to approximate this by equation 3 :-

$$S \approx \frac{R}{f} (i_2 - i_1)$$

We will later show by simulation the effects of this approximation and of a further approximation of the range equation:

$$R \approx \frac{Bf}{i_l - i_r + f(\Delta_r - \Delta_l)} \quad (7)$$

3. SYSTEM CALIBRATION

The $(\Delta_r - \Delta_l)$ term in the range equation (equation 5) may be measured by performing an underwater calibration. A target with crosshair markers on the same horizontal line and separated by the camera baseline distance, B , is used. Figure 5 shows such a target. The left camera is boresighted on the left crosshair and the distance from boresight of the right crosshair, viewed with the right camera, is noted. This is shown in Figure 6. The angle $(\Delta_r - \Delta_l)$ can be directly measured where :-

$$(\Delta_r - \Delta_l) = \arctan \frac{i_r}{f} \quad (8)$$

i_r is measured from the TV picture/signal with an operator merging images as described above.

Note that this calibration is different from simply applying a shift to the relative image offset. The $f(\Delta_r - \Delta_l)$ term in equation 5 is a shift in relative image displacement but the $\frac{i_r(\Delta_r - \Delta_l)}{f}$ term represents a shift which varies with image position.

4. SYSTEM MODELLING

System modelling was performed to examine the likely accuracy of the system using the approximated range and size equations derived earlier. The minimum required accuracy was $\pm 10\%$ at 10 m, though any improvement was considered highly beneficial. For all calculations a 1m wide target at 10 m range was assumed to be placed at 250 positions on either side (on a horizontal plane) of the left camera optical axis. This corresponds to object positions throughout the cameras' horizontal fields of view. For each object position the image position for each camera was calculated, taking into account the effects of the front-window misalignment on the cameras. These image positions were then used in the various range and size equations being modelled.

Results are shown graphically in Figures 7 to 11 with the object position plotted on the abscissa and range or size plotted on the ordinate. In all cases two examples of window misalignment are given. The leftmost plot shows the case where the left camera angular shift in the horizontal plane is -0.006 radians (-0.34 degrees), the right plot shows the case where the left camera angular shift is $+0.006$ radians. In all cases the right camera angular shift is $+0.006$ radians. Hence the right plot is the case where the rays are shifted equally for both cameras.

4.1. Simple Range Equation

Figure 7 shows the calculated range using the simple range equation given as equation 2 and the corresponding calculated size using equation 3 (which uses the calculated range) for the two cases of window misalignment described above.

Bearing in mind the true range of -10 m it can be seen that when the two cameras are not similarly misaligned the simple range formula of equation 2 is hopelessly inaccurate and varies throughout the camera horizontal field of view. The effects of this range error upon the size calculation are also apparent. The simple range formula does not meet the required accuracy.

When the cameras are similarly misaligned (right side plots) the simple range formula is accurate to approximately 0.5% . The size equation can be seen to be highly

accurate, with calculation precision effects clearly visible on the amplified scale of the plot.

4.2. Full Range and Size Formulae

To verify the full range and size formulae given as equations 4 and 6, the same simulations were performed using these formulae. The results are shown in Figure 8. For the two misalignment conditions described above this figure shows calculated range, percentage range error, calculated size and percentage size error.

The figure shows the range and size error to be no worse than 0.0006% and almost uniform throughout the field of view. This error may be due to the small angle approximation used in the equations' derivation.

The complete range and size formulae are more than adequate to meet the system accuracy requirements though as mentioned previously several terms are not readily obtainable in a practical system.

4.3. Range and Size Formula Approximations

To assess which terms of the full range formula it is possible to drop, the above simulation was run for two 'cut-down' versions of the range formula of equation 4. These were equation 7:

$$R = \frac{Bf}{i_l - i_r + f(\Delta_r - \Delta_l)}$$

and equation 5 :-

$$R = \frac{Bf}{i_l - i_r + f(\Delta_r - \Delta_l) + \frac{i_l i_r (\Delta_r - \Delta_l)}{f}}$$

Equation 7 represents the simple range formula with a shift term. Equation 5 represents the simple range formula with a shift term and an image position dependent shift term.

Figure 9 shows the calculated range and range error for these formulae and for the full range formula (equation 4) as well as size and size error using equation 3. For size calculations the range value used is the calculated range not the true range. On some graphs only two plots are apparent. In these the plots corresponding to equations 4 and 5 are coincident though with an expanded scale they would not be, with the plot for equation 5 having a similar shape to that for equation 7.

The plots for equation 7 are the least accurate with accuracy decreasing with distance from the camera optical axis. All equations meet the accuracy requirement though equation 5 offers significant improvement without requiring additional information.

As with previous results all equations are more accurate when window misalignments for the two cameras are the same.

Having shown that it is possible to derive range and size to the required accuracy using practically useable approximations to the true formulae we now consider the effect of data sampling on range and size accuracy. Since equation 5 offers an improvement over equation 7 at no expense (except for slightly more computation) this formula will be used in the further analysis.

4.4. Sampling Effects

This section identifies the likely errors arising from the use of a sampled system, i.e. a CCD TV camera. Simulations were performed as above but the calculated image position of each object position and each camera was subjected to binning. The bin size used was the dimension of a single CCD detector element. A 'calibration' was performed by similarly binning the (Δ_x, Δ_y) values for the various tilts. Following this the range using equation 5 and the size using equation 3 were calculated.

A typical CCD camera will have up to 768 elements horizontally and simulations were initially performed for 1600 object positions throughout the field of view to avoid subsampling artifacts. For the purposes of illustration the graphs presented here were produced using 500 object positions as for the earlier simulations since individual lines are not visible with 1600 plot points. The plots shown are representative of those obtained with more samples.

The top half of Figure 10 shows range and range error for the two standard tilts as used above. The effects of sampling are clearly apparent. Notice that the fluctuations in calculated range are grouped together and that a transition between groups occurs where the binning causes the image position error to 'jump' a whole pixel.

For the case where the left camera tilt is different from the right camera a distinctive bending can be observed. The sampling has in fact accentuated the bending in the basic range formula - an effect which was invisible in the non-sampled case plotted in Figure 9.

The error in range is -7.5% to +2.5% which is within the system accuracy requirements.

The lower plots in Figure 10 show how halving the bin size improves the range error. This may be achieved in practice by interpolating between adjacent image pixels using image processing techniques, assuming that the image of the ranging point spans two adjacent pixels. The range error for the smaller bin size is approximately $\pm 2.5\%$ - well within the system requirements.

It is interesting to note how in a non-sampled system and where the left and right cameras had the same tilt the range equation (equation 5) produced a symmetric plot. In a sampled system however the 'grouping' of the fluctuations in calculated range is asymmetric and varies with the tilt.

4.5. Effect of Range Calculation on Size Measurement

Throughout this section results of size measurement have been presented for various range formulae though all have used the same size formula, given as equation 3. Whilst it is clear that the range calculation has an impact upon the size calculation no quantitative assessment of this effect has been made. Presented here are the results of two simulations. One uses the range calculation of equation 5 to derive range values which are then used in the equation 3 size formula. The other uses the true (10 m) range directly in the equation 3 size calculation. In both cases sampling effects are included with the bin size equal to half the CCD detector size (i.e. we assume some interpolation).

Figure 11 gives the results of the two simulations with the normal two tilt cases for each. The upper plots show the simulation where calculated range is used in the size formula. The lower plots use the true (uncalculated and unsampled) range.

The effect of the range calculation upon the size calculation is quite clear. Both the characteristic curve (for left tilt \ll right tilt) of the range formula and the

sampling effects impose themselves upon the calculated size, as might be expected. Clearly a further improvement in the range calculation would be reflected in the size accuracy.

5. CONCLUSIONS

This report has shown how, in a practical underwater stereo ranging and sizing system, the standard range and size formulae may not be sufficiently accurate to allow useful measurements.

It has demonstrated how the effects of window misalignment may be made insignificant through the use of an electronic underwater calibration scheme and a new ranging formulation.

The effects of image sampling upon range and size accuracy have been demonstrated and now represent the major limitations upon range and size accuracy even when image pixel interpolation is allowed. It may be possible to further interpolate the stereo images to allow image matching to one quarter of a pixel (one quarter of a CCD element) accuracy but this will require further investigation.

Simulations were performed at a typical operating range of 10 m. Ranges much in excess of this are only achievable in very clear water. For such ranges the sampling effects described here will become more dominant if the camera baseline is not increased.

The theoretical results presented here are currently being tested experimentally.

6. ACKNOWLEDGMENTS

The author wishes to thank Dr C.J. Woodruff for his great assistance in the area of optical theory.

SRL-0130-TR

UNCLASSIFIED

REFERENCES

1. Gonzalez, RC & Wintz, P (1987). *Digital Image Processing*. Addison-Wesley, Reading, Mass. pp. 52-54.
2. Ballard, DH & Brown, CM (1982). *Computer Vision*, Prentice Hall, Englewood Cliffs, NJ. pp. 20-22. 88-93.
3. Weng, J (1992). *Camera Calibration with Distortion Models and Accuracy Evaluation*, IEEE Trans. on Pattern Analysis and Machine Intelligence, Vol. 14, No. 10, October 1992, pp 965-980.
4. Han, XZ (1991). *Problems of Photogrammetry of Moving Target in Water*, SPIE Vol. 1537, Underwater Imaging, Photography and Visibility. pp 215-220
5. Corena, L & Gillyon, MP. *Private Communication on results of modelling the effects of front window tilt in water medium*. Optoelectronics Division, Defence Science and Technology Organisation, Salisbury, South Australia.

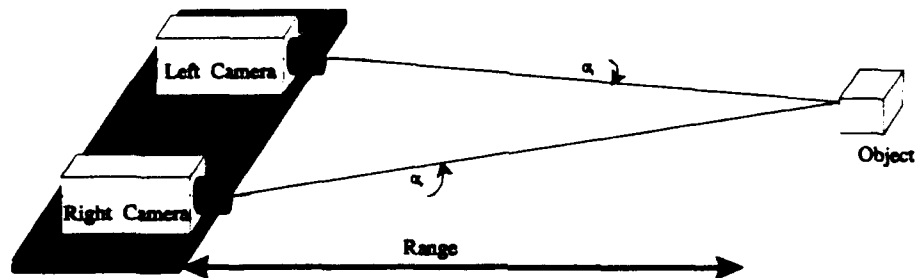


Figure 1 - Ranging With Stereo TV Cameras

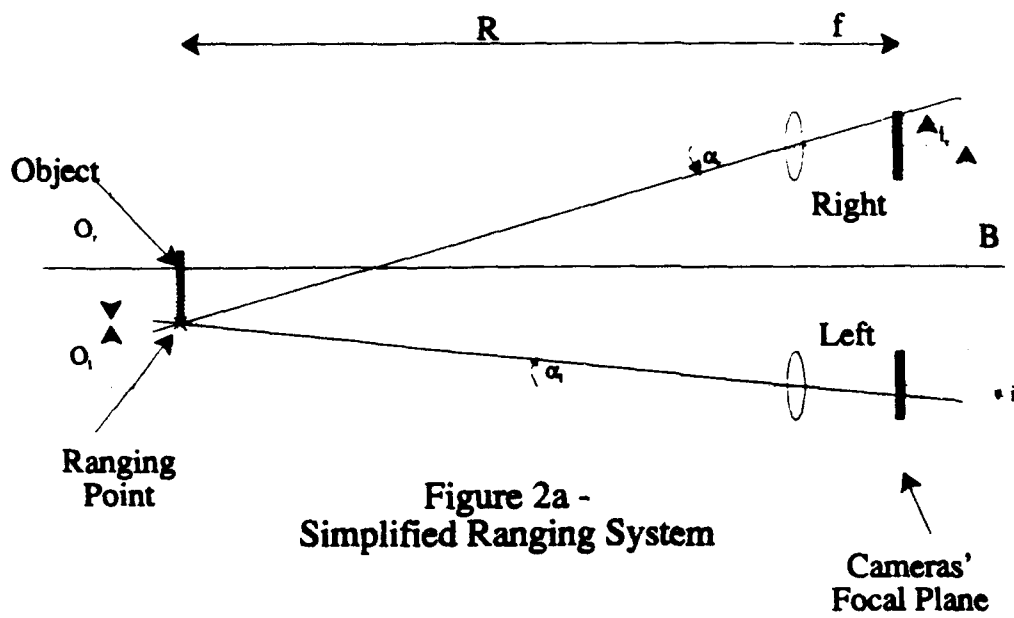
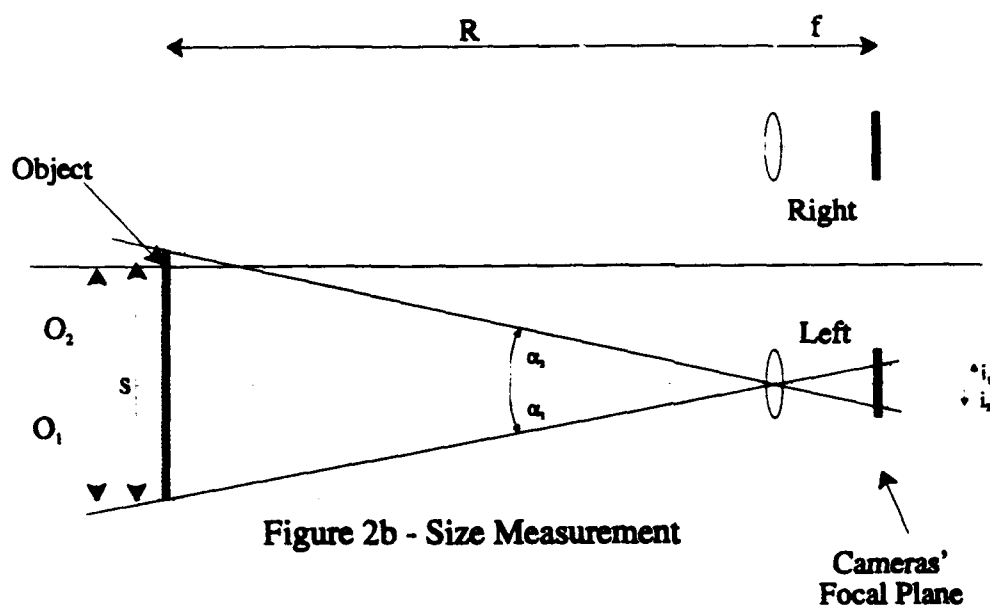
Figure 2a -
Simplified Ranging System

Figure 2b - Size Measurement

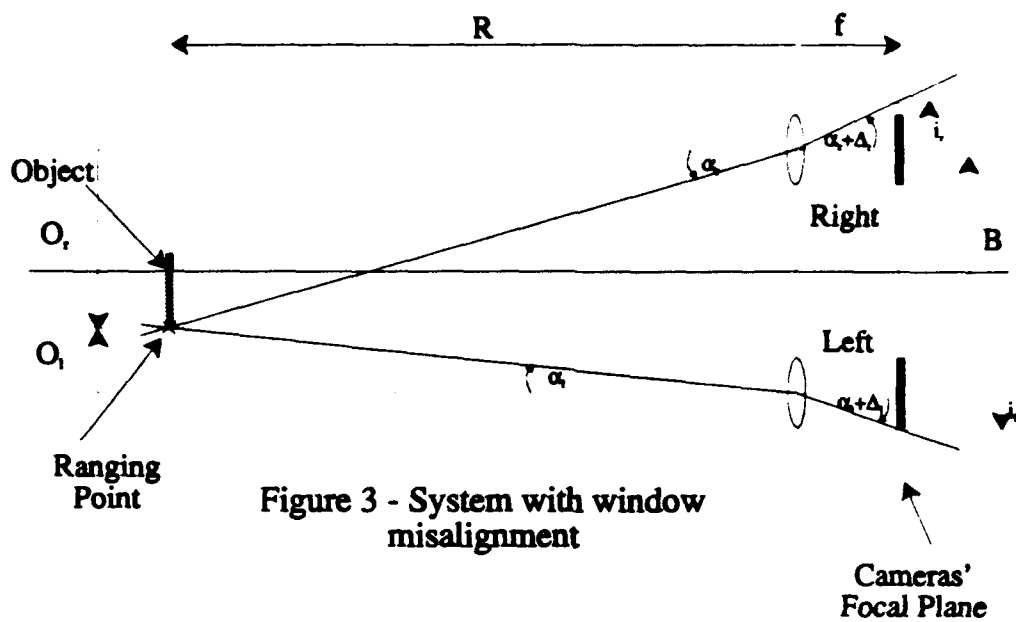


Figure 3 - System with window misalignment

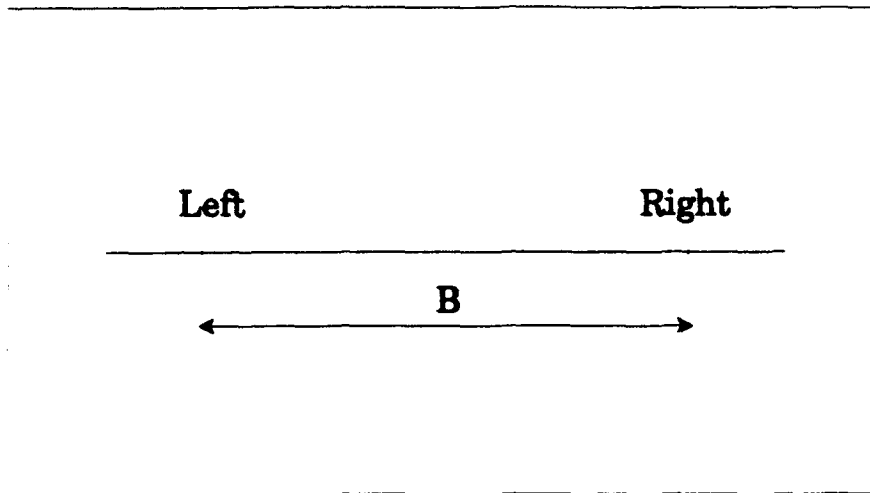
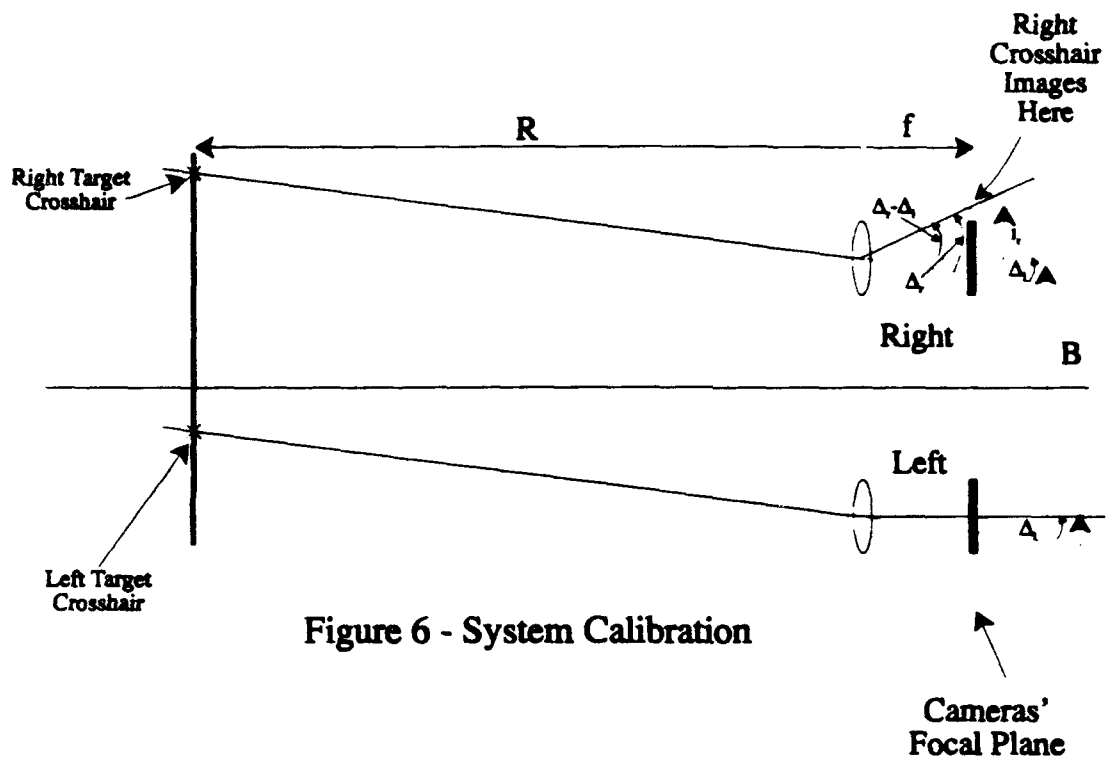
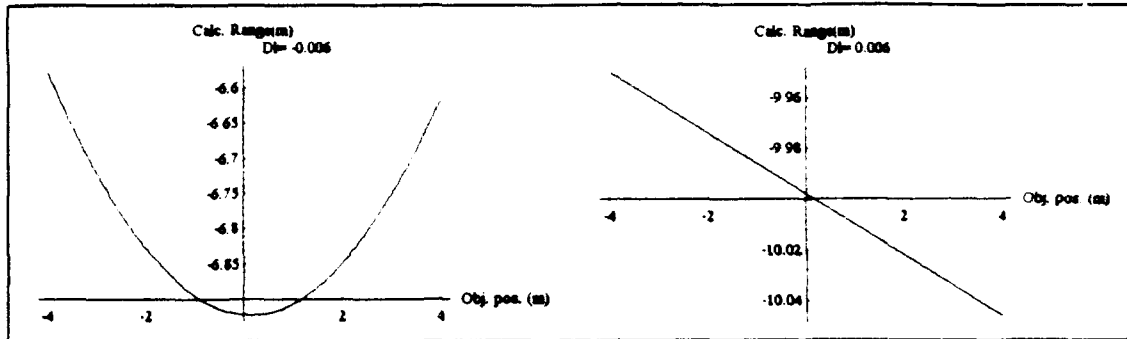
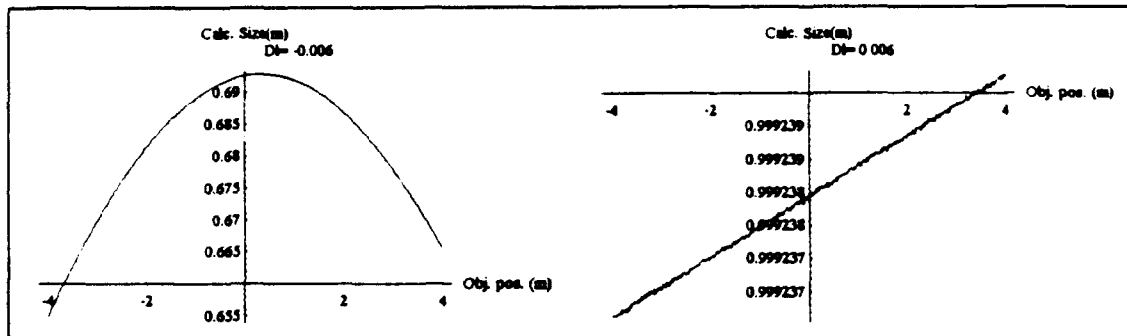


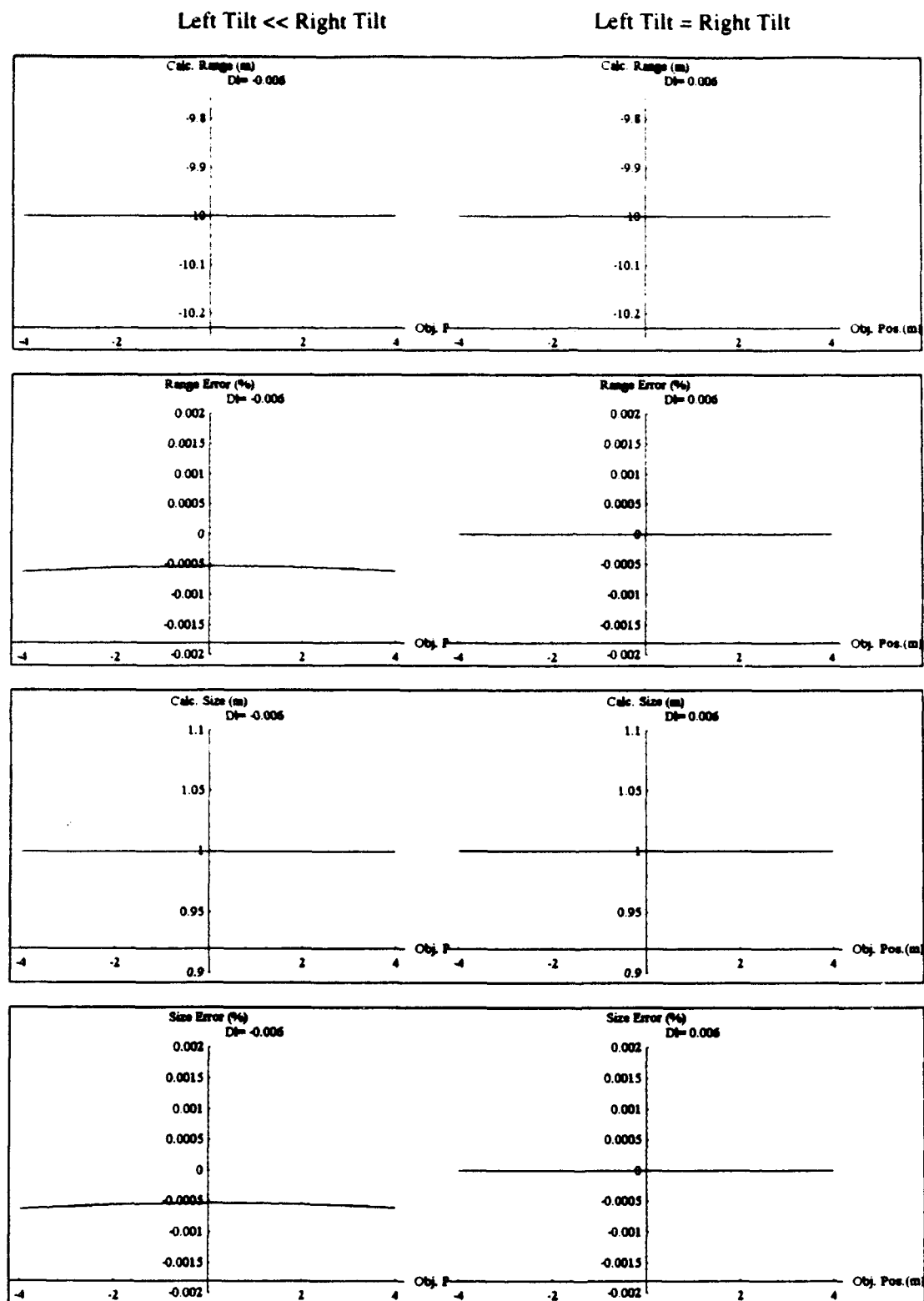
Figure 5 - Calibration Chart



Left Tilt << Right Tilt

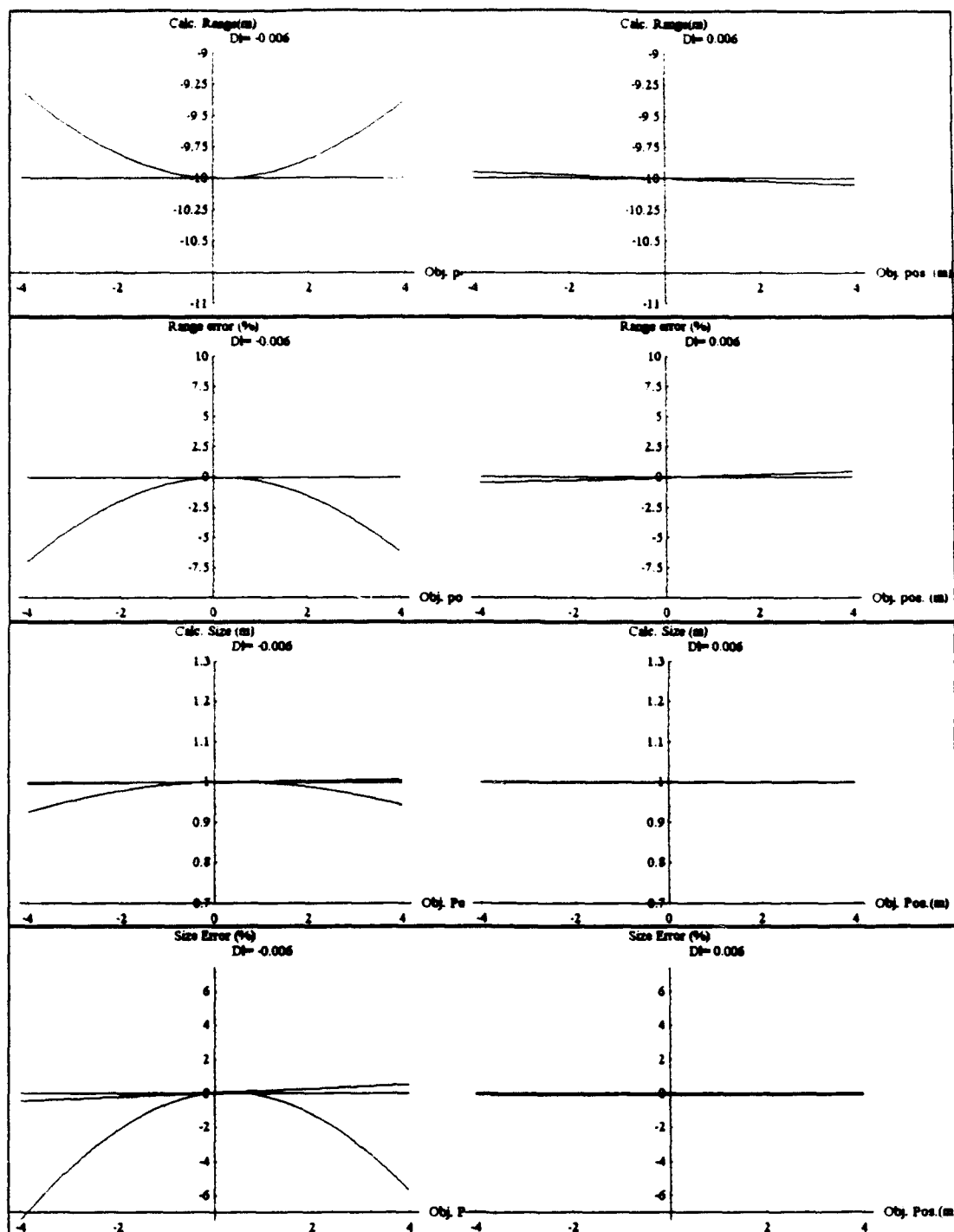
Left Tilt = Right Tilt

Calculated Range vs. Object PositionCalculated Size vs. Object Position**Figure 7 - Calculated Range and Size for the Simple Formula**

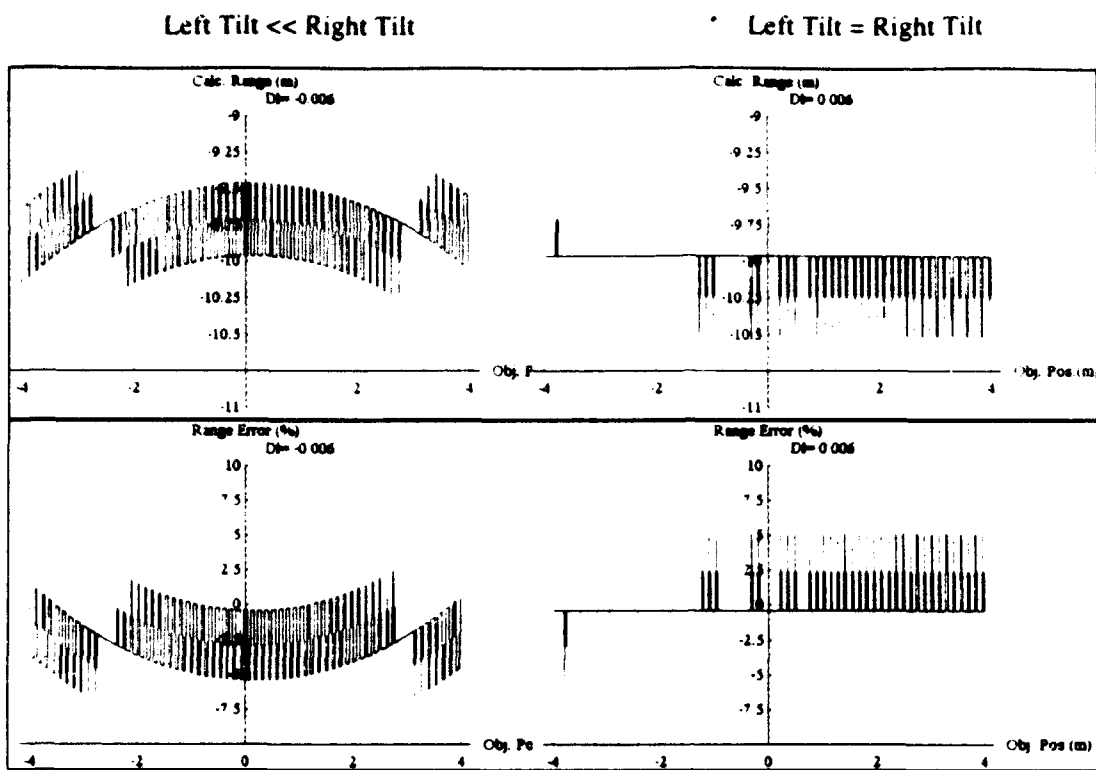
**Figure 8 - Range and Size Calculations for Full Formula**

Left Tilt << Right Tilt

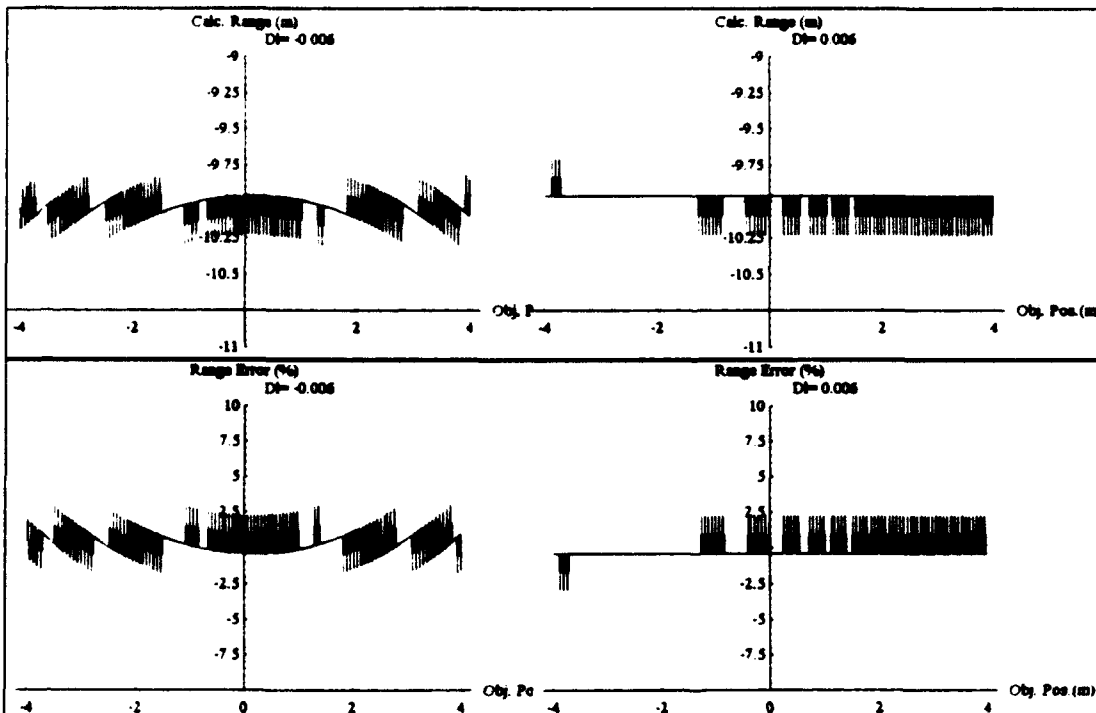
Left Tilt = Right Tilt

**Figure 9 - Comparison of Range Equations**

Range and size plots using Equations 4, 5 & 7. NOTE : Plots for equations 4 & 5 are sometimes coincident.



Large Sample Bin



Small Sample Bin

Figure 10 - Range Calculation with two Sample Sizes

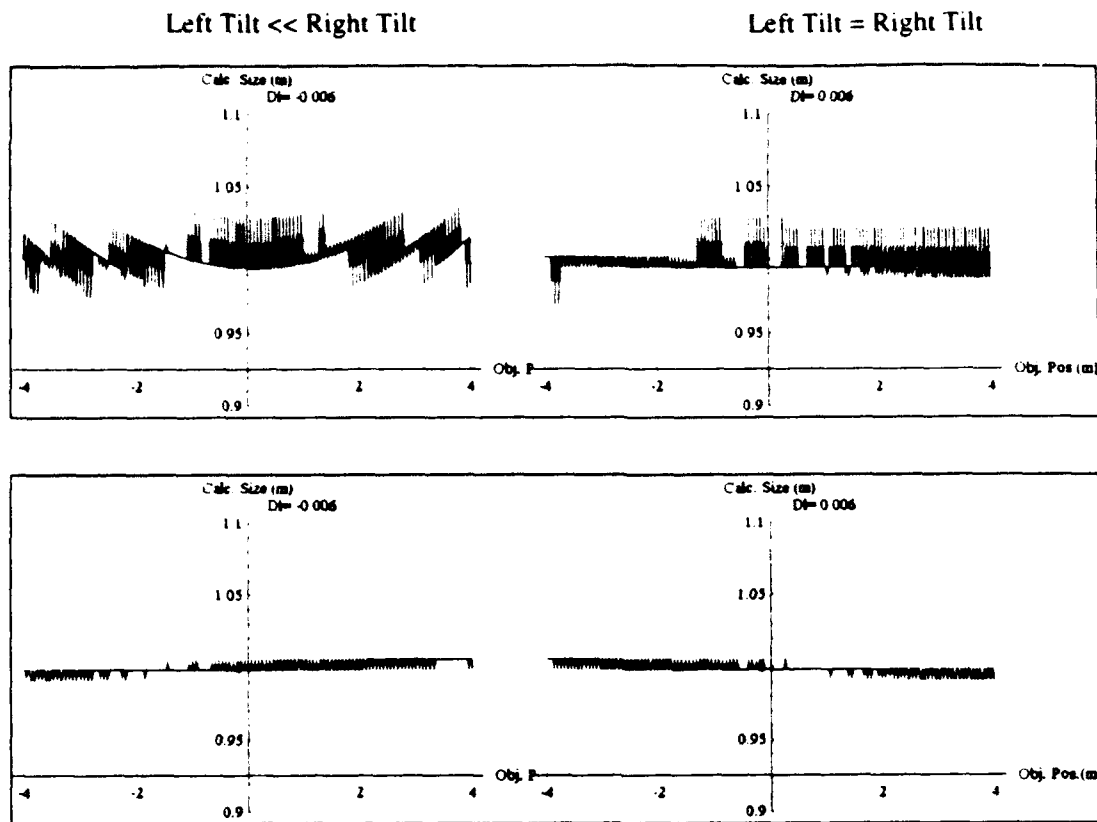


Figure 11 - Effect of Calculated Range Inaccuracy on the Size Calculation

SRL-0130-TR

UNCLASSIFIED

APPENDIX A - THEORETICAL DEVELOPMENT OF THE OPTICAL EFFECTS OF WINDOW MISALIGNMENT IN A THREE MEDIA SYSTEM

For an optical system in water we will show how the deviation in any light ray caused by a fixed tilt in the system optics front window produces a fixed angular offset in perceived angle of incidence. We also show that the shift in the position of the emergent ray is so small that it may be ignored.

Figure A1 shows a light ray travelling through three media which in our system will typically be water, glass (the front window) and air. Angles are positive anticlockwise and a conventional cartesian coordinate system is assumed. These media have refractive indices N_1 , N_2 , and N_3 . The window has thickness t and the angles of incidence and refraction are marked as θ . This system has no window tilt.

System without window tilt

Angular deviation of emergent ray.

Firstly, let $k_1 = \frac{N_1}{N_2}$ and $k_2 = \frac{N_2}{N_3}$

Also, let $T_n = \tan \theta_n$ for $n = 1, 2, 3$.

A convenient paraxial approximation to Snell's law gives:-

$$T_2 = k_1 T_1 \quad - \quad (A.1)$$

and

$$T_3 = k_2 T_2 \quad - \quad (A.2)$$

and substituting from (A.1) into (A.2)

$$T_3 = k_1 k_2 T_1 \quad - \quad (A.3)$$

Deviation in emergent ray position, Y_3

we can also say that

$$Y_3 = Y_1 + t T_2 \quad - \quad (A.4)$$

Substituting from (A.1) into (A.3)

$$Y_3 = Y_1 + t k_1 T_1 \quad - \quad (A.5)$$

Equations (A.3) and (A.5) give the angle and position of the emergent ray for a system with no window tilt. We will now consider the effects of window tilt on these parameters.

System with window tilt

Angular deviation of emergent ray.

Figure A2 shows the situation with a tilted window. Primed angles (eg θ_1') represent measurements relative to a coordinate system which has rotated with the window. Unprimed angles are measured relative to the system optical axis. Y_3 is the new value of Y_1 , due to the window tilt. The window has been rotated about the position where the incident ray impinges on the front of the window. We must establish the angular deviation in the emergent ray caused by the window tilt. From the figure, θ_1' is :

$$\theta_1' = \theta_1 - \Delta \quad (A.6)$$

where Δ is the tilt angle, positive anticlockwise.

So

$$\begin{aligned} T_1' &= \tan(\theta_1' - \Delta) \\ &= T_1 - \Delta \quad \text{in the paraxial approximation} \end{aligned} \quad (A.7)$$

Now, from (A.3) :

$$T_3 = k_1 k_2 T_1' \quad (A.8)$$

From Figure A2 we can also say :

$$\begin{aligned} T_3 &= T_1' + \tan \Delta \\ &= k_1 k_2 T_1' + \tan \Delta \end{aligned}$$

From (A.7) :

$$\begin{aligned} T_3 &= k_1 k_2 (T_1 - \Delta) + \Delta \quad \text{in the paraxial approximation} \\ &= k_1 k_2 T_1 - \Delta(k_1 k_2 - 1) \end{aligned} \quad (A.9)$$

For a water/glass/air system with $k_1 k_2 = \frac{4}{3}$

$$T_3 = k_1 k_2 T_1 - \frac{\Delta}{3}$$

Hence, comparing this result with equation (A.3), the deviation in any ray caused by the window tilt is approximately equal to 1/3 the angle of tilt and in the opposite direction. This concurs with the experimentally determined value obtained by Corena and Gillyon. Note that for an air/glass/air system there is no angular deviation caused by the window tilt. This also corresponds with field observations.

Deviation in emergent ray position, Y_3

With a tilt, referring to Figure A2, we have :

$$AB = t$$

$$AC = \frac{t}{\cos \theta_2}$$

$$\begin{aligned} CD &= AC \sin(\theta_2 + \Delta) \\ &= \frac{t \sin(\theta_2 + \Delta)}{\cos \theta_2} \\ &= \frac{t(\sin \theta_2 \cos \Delta + \cos \theta_2 \sin \Delta)}{\cos \theta_2} \\ &= t(\tan \theta_2 \cos \Delta + \sin \Delta) \\ &= t(\tan \theta_2 (1 - \sin^2 \Delta)^{\frac{1}{2}} + \sin \Delta) \end{aligned}$$

In the paraxial approximation, $\tan \theta \approx \theta \approx \sin \theta$, and $\sin^2 \theta \approx 0$, so

$$\begin{aligned} CD &= t(T_2 + \Delta) \\ &= tT_2 + t\Delta \end{aligned}$$

Hence

$$Y_3 = Y_1 + tT_2 + t\Delta$$

Using (A.1) :

$$Y_3 = Y_1 + tk_1 T_1 + t\Delta$$

Using (A.7):

$$Y_3 = Y_1 + tk_1 (T_1 - \Delta) + t\Delta$$

$$Y_3 = Y_1 + tk_1 T_1 + t\Delta(1 - k_1) \quad (\text{A.10})$$

With a water/glass/air system $k_1 \approx \frac{8}{9}$ so, comparing (A.10) with (A.5), the

shift in Y position caused by the tilted window will be approximately $\frac{\Delta t}{9}$. Using typical values of $\Delta = 1^\circ$ and $t = 0.01m$ the shift caused by the tilted window is approximately $19\mu m$ and therefore we ignore it in our modelling.

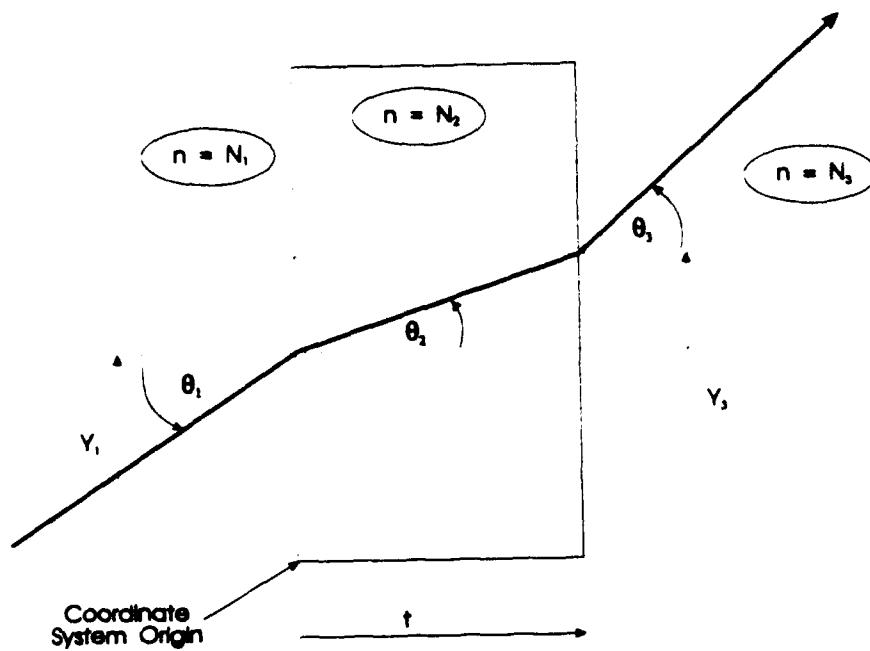


FIGURE A1 - THREE TRANSMISSION MEDIA, NO WINDOW TILT

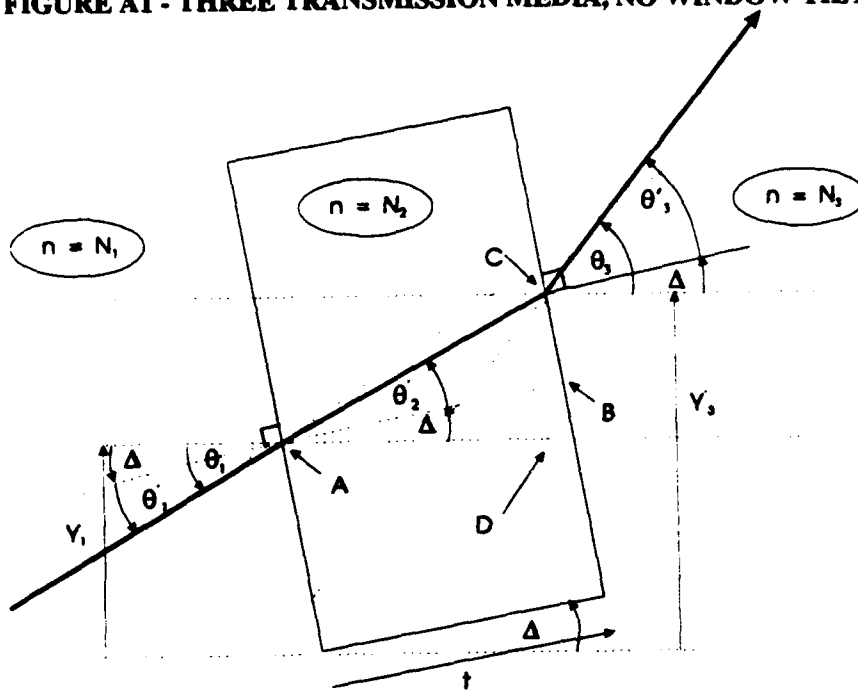


FIGURE A2 - THREE TRANSMISSION MEDIA WITH WINDOW TILT

APPENDIX B - DERIVATION OF RANGE AND SIZE FORMULAE TO INCLUDE MISALIGNMENT ERRORS

Referring to Figure 3 and using the standard formula for $\tan(A+B)$:-

$$\tan(\alpha_l + \Delta_l) = \frac{\tan\alpha_l + \tan\Delta_l}{1 - \tan\alpha_l \tan\Delta_l} = \frac{i_l}{f}$$

$$\text{So, } \frac{i_l}{f} \cdot \frac{i_l \tan\alpha_l \tan\Delta_l}{f} = \tan\alpha_l + \tan\Delta_l$$

$$\frac{i_l}{f} - \tan\Delta_l = \tan\alpha_l \left(1 + \frac{i_l \tan\Delta_l}{f} \right)$$

$$\text{and } \tan\alpha_l = \frac{\frac{i_l}{f} - \tan\Delta_l}{\left(1 + \frac{i_l \tan\Delta_l}{f} \right)}$$

Empirical measurements have shown that $\Delta_l < 1^\circ$ and so the approximation $\tan\Delta_l = \Delta_l$ is valid. Hence :-

$$\tan\alpha_l = \frac{\frac{i_l}{f} - \Delta_l}{\left(1 + \frac{i_l \Delta_l}{f} \right)} \quad (\text{B.1})$$

And similarly for $\tan\alpha_r$,

$$\tan\alpha_r = \frac{\frac{i_r}{f} - \Delta_r}{\left(1 + \frac{i_r \Delta_r}{f} \right)} \quad (\text{B.2})$$

Derivation of Range Equation

Recalling equation (1) :-

$$R = \frac{B}{\tan\alpha_l - \tan\alpha_r}$$

Substituting (B.1) and (B.2) into (1) :-

$$R = \frac{B}{\frac{\frac{i_l}{f} - \Delta_l}{\left(1 + \frac{i_l \Delta_l}{f} \right)} - \frac{\frac{i_r}{f} - \Delta_r}{\left(1 + \frac{i_r \Delta_r}{f} \right)}}$$

From which we can obtain:

$$R = \frac{B \left(f + i \Delta_r + i \Delta_l + \frac{i i \Delta \Delta_r}{f} \right)}{i_l - i_r + f(\Delta_r - \Delta_l) + \frac{i i_r (\Delta_r - \Delta_l)}{f} + \Delta_r \Delta_l (i_l - i_r)}$$

(4)

The formula for the object range.

Derivation of Size Formula

From figure 4, the object size, S is :-

$$S = O_2 - O_1$$

Using the same form of derivation as for equation (3), we obtain:

$$S = R(\tan \alpha_2 - \tan \alpha_1) \quad (\text{B.3})$$

We can also say :-

$$\frac{i_l}{f} = \tan(\alpha_l + \Delta_l)$$

and using the derivations for $\tan \alpha_l$ and $\tan \alpha_r$, we can obtain :-

$$\tan \alpha_l = \frac{\frac{i_l}{f} - \Delta_l}{\left(1 + \frac{i_l \Delta_l}{f} \right)}$$

and similarly for $\tan \alpha_2$.

$$\tan \alpha_2 = \frac{\frac{i_2}{f} - \Delta_l}{\left(1 + \frac{i_2 \Delta_l}{f} \right)}$$

Substituting into (B.3) we obtain :-

$$\begin{aligned} S &= R \left(\frac{\frac{i_2}{f} - \Delta_l}{\left(1 + \frac{i_2 \Delta_l}{f} \right)} - \frac{\frac{i_l}{f} - \Delta_l}{\left(1 + \frac{i_l \Delta_l}{f} \right)} \right) \\ &= R \left(\frac{\left(\frac{i_2}{f} - \Delta_l \right) \left(1 + \frac{i_l \Delta_l}{f} \right) - \left(\frac{i_l}{f} - \Delta_l \right) \left(1 + \frac{i_2 \Delta_l}{f} \right)}{\left(1 + \frac{i_2 \Delta_l}{f} \right) \left(1 + \frac{i_l \Delta_l}{f} \right)} \right) \\ &= R \left(\frac{\frac{i_2}{f} + \frac{i_l i_2 \Delta_l}{f^2} - \Delta_l - \frac{i_l \Delta_l^2}{f} - \frac{i_2}{f} - \frac{i_l i_2 \Delta_l}{f^2} + \Delta_l + \frac{i_2 \Delta_l^2}{f}}{1 + \frac{i_l \Delta_l}{f} + \frac{i_2 \Delta_l}{f} + \frac{i_l i_2 \Delta_l^2}{f^2}} \right) \end{aligned}$$

Simplifying and multiplying top and bottom by f :-

$$S = R \left(\frac{i_2 \cdot i_1 + \Delta_f^2 (i_2 \cdot i_1)}{f + \Delta_f (i_1 + i_2) + \frac{i_1 i_2 \Delta_f^2}{f}} \right) \quad (6)$$

The formula for the object size.

SRL-0130-TR

UNCLASSIFIED

- 30 -

UNCLASSIFIED

DISTRIBUTION

	No of Copies
Defence Science and Technology Organisation	
Chief Defence Scientist)	
Central Office Executive)	1 shared
Director General, Science Policy Development	1
Director, International Programmes	1
Counsellor, Defence Science, London	Cont. Sht.
Counsellor, Defence Science, Washington	Cont. Sht.
Senior Defence Scientific Adviser	1
Navy Scientific Adviser	1
Air Force Scientific Adviser	1
Scientific Adviser, Army	1
Scientific Adviser, Policy and Command	1
Assistant Secretary, Scientific Analysis	1
Defence Intelligence Organisation	
Director, Science and Analysis, DIO	1
Surveillance Research Laboratory	
Director	1
Chief, Land, Space & Optoelectronics Division	1
Chief, Microwave Radar Division	Cont. Sht.
Chief, High Frequency Radar Division	Cont. Sht.
Research Leader Space and Surveillance Systems	1
Research Leader Land	1
Head, Information & Image Processing Discipline	1
Author : Mr SJ Sutherland	5
Maritime Operations Division, MRL,	
attn: D.R. Skinner	1
Media Services	1
Libraries and Information Services	
Australian Government Publishing Service	1
Defence central Library, Technical Reports Centre	1
Manager, Document Exchange Centre, (for retention)	1
National Technical Information Service, United States	2
Defence Research Information Centre, United Kingdom	2
Director Scientific Information Services, Canada	1
Ministry of Defence, New Zealand	1
National Library of Australia	1
Defence Science and Technology Organisation Salisbury, Research Library	2
Defence Science and Technology Organisation MRL Research Library	1
Defence Science and Technology Organisation ARL Research Library	1
Library Defence Signals Directorate, Melbourne	1
British Library Document Supply Centre	1
Spares	
Defence Science and Technology Organisation Salisbury, Research Library	6

SRL-0130-TR

UNCLASSIFIED

- 32 -

UNCLASSIFIED

Department of Defence
DOCUMENT CONTROL DATA SHEET

1. Page Classification UNCLASSIFIED			2. Privacy Marking/Caveat (of document) N/A		
3a. AR Number AR-008-170	3b. Laboratory Number SRL-0130-TR	3c. Type of Report TECHNICAL REPORT	4. Task Number 92/218		
5. Document Date October 1994 3	6. Cost Code 802774	7. Security Classification <div style="display: flex; justify-content: space-around;"> <div style="border: 1px solid black; padding: 2px;">U</div> <div style="border: 1px solid black; padding: 2px;">U</div> <div style="border: 1px solid black; padding: 2px;">U</div> </div> Document Title Abstract	8. No. of Pages 36	9. No. of Refs. 5	
10. Title ANALYSIS AND COMPENSATION FOR WINDOW ALIGNMENT ERRORS IN AN UNDERWATER STEREO TV CAMERA RANGING AND SIZING SYSTEM		* For UNCLASSIFIED docs with a secondary distribution LIMITATION, use (L) in document box.			
		S (Secret) C (Confl) R (Rest) U (Unclass)			
11. Author(s) S. J. Sutherland		12. Downgrading/Delimiting Instructions N/A			
13a. Corporate Author and Address Surveillance Research Laboratory PO Box 1500, Salisbury SA 5108		14. Officer/Position responsible for Security:..... N/A Downgrading:..... N/A Approval for Release:..... DSRL			
13b. Task Sponsor NAV					
15. Secondary Release Statement of this Document APPROVED FOR PUBLIC RELEASE					
16a. Deliberate Announcement No limitation					
16b. Casual Announcement (for citation in other documents) <div style="display: flex; justify-content: space-around;"> <input checked="" type="checkbox"/> No Limitation <input type="checkbox"/> Ref. by Author , Doc No. and date only. </div>					
17. DEFTTEST Descriptors Stereophotography, Television cameras, Underwater cameras, Alignment, Measurement, Errors, Distance, Calibration			18. DISCAT Subject Codes 1404		
19. Abstract This report considers the theoretical analysis of measurement errors introduced in an underwater stereopsis system which has front window misalignment. It develops new range and size equations and models the effects of window misalignment, range equation approximation and system sampling effects. A scheme is given which will allow underwater calibration in a practical system. The report concludes that the new range and size equations developed provide enhanced accuracy to a point where the system sampling effects become the dominant source of error.					